ELSEVIER

Journal of Physics and Chemistry of Solids 61 (2000) 1639–1645

JOURNAL OF PHYSICS AND CHEMISTRY OF SOLIDS

www.elsevier.nl/locate/jpcs

Electronic structure calculations of PbTe

M. Lach-hab[a,b], M. Keegan[b], D.A. Papaconstantopoulos[b,c,*], M.J. Mehl[c]

[a]*Department of Materials Science and Engineering, Virginia Polytechnic Institute and State University, Blacksburg, VA 24061-0237, USA*
[b]*Institute for Computational Sciences and Informatics, George Mason University, Fairfax, VA 22030-4444, USA*
[c]*Center for Computational Materials Science, Naval Research Laboratory, Washington, DC 20375, USA*

Received 19 January 2000; accepted 27 January 2000

Abstract

The full potential linearized augmented plane wave (LAPW) method was applied to study the electronic structure of the PbTe compound. Calculations of the band structure, density of states, strain energy and total energy as a function of lattice constant have been performed in the B1(NaCl) and B2(CsCl) structures. The equilibrium lattice constant, the band gap, the pressure variation of the energy gap, the bulk moduli and the elastic constants are compared with experiment and other calculations. We found that the local density approximation results in an energy gap that overestimates the experimental value, in contrast to most materials where the energy gap is underestimated. We propose a simple way to adjust the gap to the experimental value by performing a Slater–Koster fit and then varying the *p* on-site parameter of Pb. The inclusion of the spin–orbit coupling term in the tight-binding Hamiltonian fit is shown to produce significant changes in the band structure. With these two steps, the calculated band gap is found to be in good agreement with experiment. In the case of PbTe (CsCl) structure, our calculation finds no gap in the bands, contradicting recent experimental data.

Keywords: A. Chalcogenides; D. Electronic structure; D. Semiconductivity

1. Introduction

Over the past several decades, the naturally occurring semiconductor PbTe has been the subject of many theoretical [1–12] and experimental [15–23] studies. Lead telluride (PbTe), with a direct and narrow band gap, was viewed as an important technological material [20–23] for a wide of variety applications in infrared devices. This compound crystallizes in the rock salt structure. Extensive calculations of the band structure of this material have been carried out using different methods, such as the tight-binding method (TB) [1], augmented-plane wave (APW) [2,4], Green's function method [5], orthogonalized plane wave (OPW) [6], and the empirical-pseudopotential methods [7–11].

Recently, a theoretical analysis of experiments [18] was presented by Wei and Zunger [12] using the linear augmented plane wave (LAPW) method [13]. A common feature of the experimental results and the theory is the existence of the band gap at the *L* point of the Brillouin zone. Wei and Zunger adjusted their potential to reproduce the exact value of the measured gap.

In this work we wish to investigate the size of the gap without the adjustment made by Wei and Zunger [12] and then explore a simple way for adjusting the gap via TB theory. We want to explore this compound in the CsCl structure in view of recent experiments [19] that propose a semiconducting phase.

This paper deals with electronic structure calculations carried out on the PbTe compound and is organized as follows. In Section 2, we outline the computational details used to obtain the equilibrium lattice constant, elastic constants and the energy gap. Also we outline the treatment of the spin–orbit interaction by means of the Slater–Koster (SK) fit approach. In Section 3 we present the results of LAPW calculations for PbTe in its stable B1 (NaCl) and in its potentially metastable B2 (CsCl) structure. We compare our calculation with experiment and

* Corresponding author. Center for Computational Materials Science, Naval Research Laboratory, Washington D.C. 20375, USA. Fax: +1-202-404-7546.

E-mail address: papacon@dave.nrl.navy.mil (D.A. Papaconstantopoulos).

0022-3697/00/$ - see front matter
PII: S0022-3697(00)00045-7

previous theoretical results. The results of the band structure from SK fit, including spin–orbit coupling, are also presented. Finally in Section 4 we summarize our conclusions.

2. Method

The band structure calculations were performed self-consistently using the general potential LAPW method [13,14], in which the core electrons, (Pb, Xe core + 4f states) (Te, Kr core + 4d states), are determined for each iteration by a fully relativistic atomic-like calculation, and the outer valence electrons were calculated scalar relativistically without spin–orbit coupling. The total energy was calculated from the usual local density approximation (LDA) expression using the Hedin and Lundqvist [24] exchange and correlation parametrization. Convergence was assumed when the total energies of two successive iterations agreed to within 10^{-5} Ry.

We performed a calculation of the total energy as a function of volume for PbTe in both the NaCl and CsCl structures. In addition, the stability of these phases was considered by calculating the elastic constants. To do this we applied an external strain to the crystal (within the elastic limit), and determined the elastic constants by calculating the curvature of the total energy as function of strain. Three independent elastic moduli, C_{11}, C_{12} and C_{44}, are needed to describe the elasticity in a cubic crystal. A more detailed descriptions of how to obtain elastic constants is presented by Mehl et al. [25,26].

It is well known that in semiconductors the band gap is not calculated accurately by the LDA. This is a shortcoming of the LDA which is magnified in our LAPW calculations by the omission of the spin–orbit interaction. To improve our band gap result we first performed a SK [30] fit using an orthogonal basis set of s and p orbitals. We followed a procedure similar to that described in Ref. [31] which we summarize later.

We used an orthogonal sp^3 TB Hamiltonian which results in an 8×8 secular equation. We used as adjustable parameters 32 three-center interaction integrals, which include first and second neighbors. These parameters were determined by a nonlinear least-squares fit to the muffin-tin (MT) APW results. In this way, we have fit all 8 bands of the MT APW calculations. The rms fitting error was less than 5 mRy for all bands.

In the SK fit it is necessary to block-diagonalize the Hamiltonian at high symmetry points and lines. For this reason, we needed to identify unambiguously the symmetry of each first principles eigenvalue to be fitted. This is done conveniently in our MT APW program. We then compared the resulting energy bands between full potential LAPW and MT APW and found that the differences are negligible. It should be noted, however, that the MT approach did not produce satisfactory total energy results [32].

Table 1
SK parameters, orthogonal 3-center, B1 structure. On the left side column we show the notation used in Tables A2 and A3

	(Ry)		
A_1	−0.32924	$s,s(000)$	Pb–Pb
A_6	0.36711	$x,x(000)$	Pb–Pb
A_2	−0.00031	$s,s(110)$	Pb–Pb
A_3	0.01505	$s,x(110)$	Pb–Pb
A_7	0.00981	$x,x(110)$	Pb–Pb
A_8	−0.01164	$x,x(011)$	Pb–Pb
A_9	0.02258	$x,y(110)$	Pb–Pb
B_1	0.00462	$s,s(200)$	Pb–Pb
B_2	−0.00799	$s,x(200)$	Pb–Pb
B_4	0.05192	$x,x(200)$	Pb–Pb
B_5	0.00265	$y,y(200)$	Pb–Pb
C_1	−0.44055	$s,s(000)$	Te–Te
C_2	−0.00112	$s,s(110)$	Te–Te
C_3	−0.00519	$s,x(110)$	Te–Te
C_6	0.17412	$x,x(000)$	Te–Te
C_7	−0.00501	$x,x(110)$	Te–Te
C_8	0.01215	$x,x(011)$	Te–Te
C_9	−0.00097	$x,y(110)$	Te–Te
E_1	−0.01524	$s,s(200)$	Te–Te
E_2	−0.00876	$s,x(200)$	Te–Te
E_4	−0.01514	$x,x(200)$	Te–Te
E_5	0.00479	$y,y(200)$	Te–Te
D_1	−0.02592	$s,s(100)$	Pb–Te
D_2	−0.04522	$s,x(100)$	Pb–Te
D_3	−0.10260	$x,s(100)$	Pb–Te
D_4	−0.10422	$x,x(100)$	Pb–Te
D_5	0.04047	$y,y(100)$	Pb–Te
F_1	−0.00462	$s,s(111)$	Pb–Te
F_2	−0.00000	$x,s(111)$	Pb–Te
F_3	0.00658	$s,x(111)$	Pb–Te
F_4	−0.00348	$x,x(111)$	Pb–Te
F_5	−0.00068	$x,y(111)$	Pb–Te

In the above fit, we did not take into account the spin–orbit coupling effect. To address this issue we included the spin–orbit coupling in the SK formalism of the TB theory. The Hamiltonian was doubled in size, that is, a 16×16 matrix is diagonalized to obtain the energy bands and density of states.

The Hamiltonian matrix expression in the angular momentum representation can be found in a review by Hass et al. [29] which we write in the form:

$$\tilde{H}+\tilde{H}_{so}=\begin{pmatrix} H+H_{so}(\uparrow\uparrow) & H_{so}(\uparrow\downarrow) \\ H_{so}(\downarrow\uparrow) & H+H_{so}(\downarrow\downarrow)\end{pmatrix} \quad (1)$$

We give the detailed form of this Hamiltonian in Appendix A (Tables A1–A3). The values of the two spin–orbit parameters of the atoms Pb and Te, λ_1 and λ_2, were taken from Herman's atomic structure calculations [28]. The remaining SK parameters that appear in the matrix elements of Tables A2 and A3 were determined from the SK fit described above and are listed in Table 1.

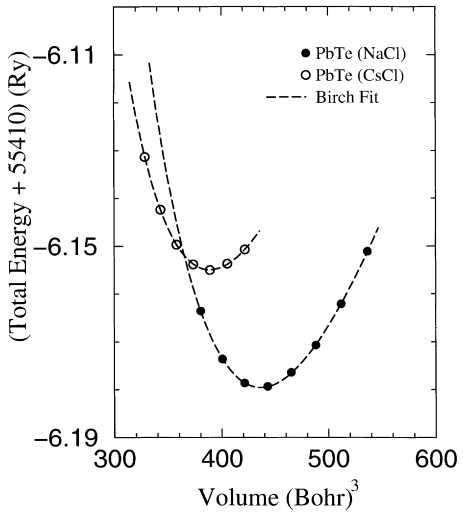

Fig. 1. Energy vs volume for the B1 and B2 structures of PbTe. The full and open circles represent the LAPW calculated energies while the dashed lines are the fits to the Birch equation of state.

In the case of the (B2) structure we included the d-states in our SK Hamiltonian to eliminate any uncertainties regarding the existence of a gap.

3. Results

Using the full-potential LAPW formalism, we have calculated the equilibrium lattice constant of PbTe within the LDA approximation. In Fig. 1 we show the total energy as a function of volume in the (B1) and (B2) structures, as well as the energy curve produced from the fit model equation of state proposed by Birch [33]. It is clear that B1 is the stable structure. The equilibrium lattice constants, bulk modulus and the first derivative of the bulk modulus, along with the corresponding experimental [18] and other calculated values [12] are listed in Table 2. The lattice parameter value is compared to the experimental value and to the Wei and Zunger value. The small difference in the value of the lattice constant between our value and that of Wei and Zunger is probably due to the fact that they used the Ceperley–Alder exchange and correlation functional as parameterized by Perdew and Zunger [34] while we have used Hedin–Lundqvist [24]. The bulk moduli agree well between the two calculations and they both are significantly higher than the experimental value of 0.400 Mbar. The value of the bulk modulus 0.477 Mbar is obtained when it is determined at the experimental volume. This is an improvement from the value 0.517 Mbar at the theoretical equilibrium volume, which is smaller than the experimental volume.

Table 2
Summary of experimental, Wei and Zunger and our calculations for PbTe. a_{eq}, B, and B' are lattice constant, bulk modulus, and its pressure derivative, respectively, of the B1 structure

PbTe	Calc. (Wei and Zunger)	Expt. (Nimtz and Schlicht)	Calc. (present results)
a_{eq} (Å)	6.44	6.43	6.37
B (Mbar)	0.517	0.400	0.514
B'	4.52		4.08

Table 3
Elastic constants

	C_{11} (Mbar)	C_{12} (Mbar)	C_{44} (Mbar)
B1 (NaCl) (LAPW)	1.535	0.004	0.150
B1 (NaCl) (expt) [3]	1.069	0.090	0.131
B2 (CsCl) (LAPW)	0.662	0.441	0.181

We have also calculated the elastic moduli for both structures at the equilibrium lattice constants. In Table 3, we list the calculated and experimental [3] values of the elastic constants. Our calculations overestimate the values of elastic constants, consistent with the overestimation of the bulk modulus. This discrepancy is reduced when we calculate the C_{ij} at the experimental value of the lattice parameter. There are no experimental data available for the elastic constants of PbTe in CsCl (B2) structure, but these calculations may serve as a prediction. Our calculated positive value of the elastic constants is indicative of the stability of this compound in both NaCl (B1) and CsCl (B2) structure. To predict the metastability of the B2 (CsCl) structure we would also need to perform phonon frequency calculations.

For the PbTe stable B1(NaCl) structure, the energy bands were calculated at the lattice constant 6.45 Å, which is very close to the experimental value. From this calculation we confirm the observation obtained by experimental [18] and theoretical [4,12,7,8] studies which locates the gap for the PbTe system at the L point. But the energy gap is found to be 0.642 eV in comparison with the Nimtz–Schlicht experimental energy gap of 0.190 eV. This is an unusual result because in most materials the LDA approximation underestimates the energy gap [35,36]. Wei and Zunger have included spin–orbit to their LAPW calculation and they have also adjusted the energy gap to the experimental value by adding a constant potential to the conduction band states.

As discussed in Section 2, in order to include the spin–orbit coupling and to adjust the gap we have performed a SK fit. When we include the spin–orbit interaction the band structure obtained is in good agreement with Wei and Zunger. The energy gap was found to be $E_g = 0.087$ eV which is smaller than the experimental value. Then we used a simple way of adjusting the gap to the experimental value of 0.19 eV using the SK fit, i.e. we shifted the p Pb on-site parameter $x, x(000)$ to match the

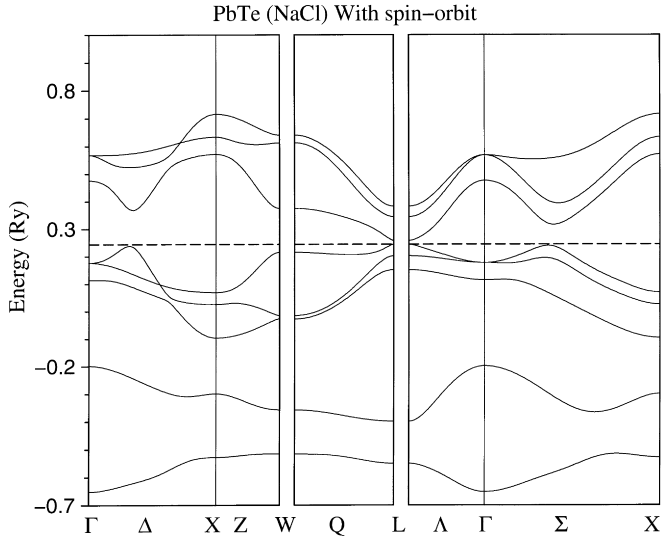

Fig. 2. The band structure along the symmetry lines of the BZ for PbTe (B1) at the lattice constant $a = 6.45$ Å. These bands were calculated with the SK parameters of Table 1. Spin–orbit effects are included.

experiment. This adjustment changes this parameter from an original value of 0.36711 Ry (4.995 eV) to the value 0.37635 Ry (5.121 eV). This procedure shows that the elimination of d states in our SK calculations is reasonable and gives an efficient way to determine the DOS of the PbTe (B1) structure. The energy bands obtained from our adjusted fit are shown in Fig. 2. The bands near the Fermi level (E_F) are predominantly a mixture of p states. The lowest band has exclusively s-Te character while the next band has s-Pb character and lies far below the gap. This, as was pointed out by Wei and Zunger, is in contrast to the situation in the conventional zinc-blende structure semiconductors, which have the cation s-band unoccupied.

In Table 4 our calculated energy gap at the symmetry points L and Γ is compared with the experimental and the theoretical values. Our LAPW value (5.38 eV) for the energy gap at Γ is found to be quite different from Wei and Zunger calculated value (3.92 eV), this is due to the effect of spin–orbit coupling used in the later calculation. But when the spin–orbit coupling is included using the SK fit an energy gap of 3.956 eV at Γ is obtained. In addition the adjustment made to improve the energy band gap at L leads to an energy gap value of 4.07 eV at Γ. This value is still in agreement to within 4% of the Wei and Zunger value.

Table 4
Energy gap values for PbTe near L and Γ

PbTe	Calc. (Wei and Zunger)	Expt. (Nimtz and Schlicht)	FLAPW	SK-fit (with spin–orbit)
$E_g(L)$ (eV)	0.19	0.19	0.64	0.087
$E_g(\Gamma)$ (eV)	3.92		5.35	3.950
$\frac{dE_g(L)}{dP}$ (eV/Mbar)	−4.01	−7.4	−6.20	

Fig. 3 shows the total density of B1 PbTe at $a = 6.45$ Å. The lower four panels show the angular momentum, site decomposed DOS. The site decomposed DOS of Fig. 3. (bottom 4 panels) reveals the origin of the main features of the DOS. The p-character states of Pb and Te dominate

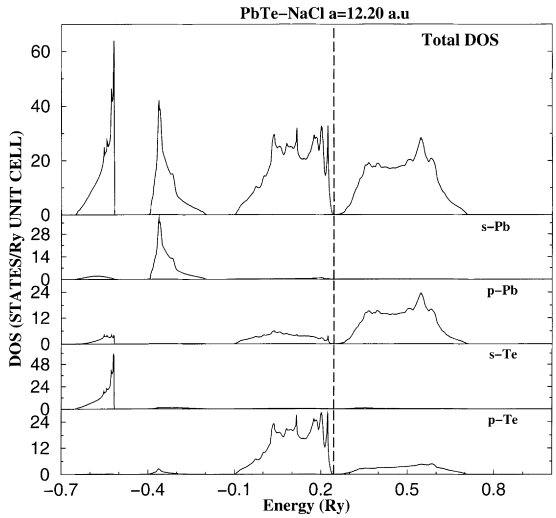

Fig. 3. Total and angular momentum-decomposed densities of states for PbTe (B1) at the lattice constant $a = 6.45$ Å, derived from our SK Hamiltonian. The position of the Fermi level is shown by the dashed vertical line. The lower panels show the partial density of states at each atom site, decomposed by the angular momentum of the state.

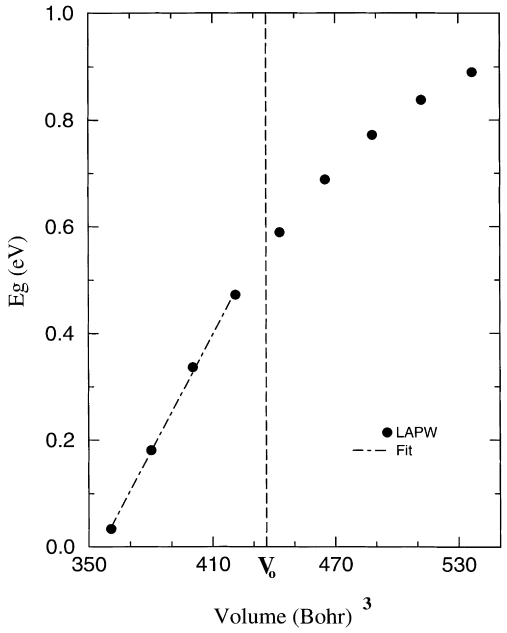

Fig. 4. Calculated volume dependent energy gap for PbTe (B1). The pressure coefficient is determined in the linear region, i.e. below the equilibrium volume $V_o = 436.3$ Bohr^3.

the total DOS near the gap and are responsible for the peaked structure shape within 6 eV above and 5 eV below the gap. The site decomposed DOS for the s-character states of Pb and s-character states of Te show a single peak feature located at 8 and 10 eV below E_F, respectively.

Fig. 4 shows the volume dependence on the energy gap of PbTe (B1). Between the lattice constant 11.3 Å and equilibrium lattice constant, the energy gap is almost linearly dependent on volume with a slope $\partial E/\partial V = 0.0073$. For lattice constants higher than that of the equilibrium the volume dependence is not quite linear. The pressure coefficient is determined when we increase the pressure, that is, from the linear region of the energy gap versus the volume. The pressure coefficient, $\partial E/\partial P$, is found to be -6.20 eV/Mbar. The experiment gives the pressure coefficient to be -7.4 eV/Mbar. The fact that the pressure coefficient is computed with reasonable agreement to the experiment indicates that the spin orbit effect would be uniform as a function of volume. It is worth noting from Table 4, $\partial E/\partial P$ value of Wei and Zunger is significantly lower than the experimental value.

Finally a proposed metastable PbTe in the (CsCl) structure with a gap of 0.21 eV was measured by Baleva and Mateeva using transmittance and reflectance spectra. A recent calculation [32] using the APW method and the calculations performed here find no gap in the bands, as shown in Fig. 5, disagreeing with these experiments. The experimental results indicate that the volume is reduced by 30% due to the pressure involved in creating the metastable CsCl phase but we find no gap for all lattice constants we calculated.

4. Conclusions

In this paper, we have performed LAPW calculations of the PbTe energy bands in the B1 and B2 structure. The calculated equilibrium lattice constant and the bulk moduli in the (NaCl) structure agree well with the experiment and calculated values of Wei and Zunger. The energy gap is reproduced accurately only by constructing an orthogonal s, p basis SK Hamiltonian with the spin–orbit coupling included and varying the p on-site parameter of Pb. The predictions are then consistent with existing experimental data and the stable structure of the PbTe. Our calculations

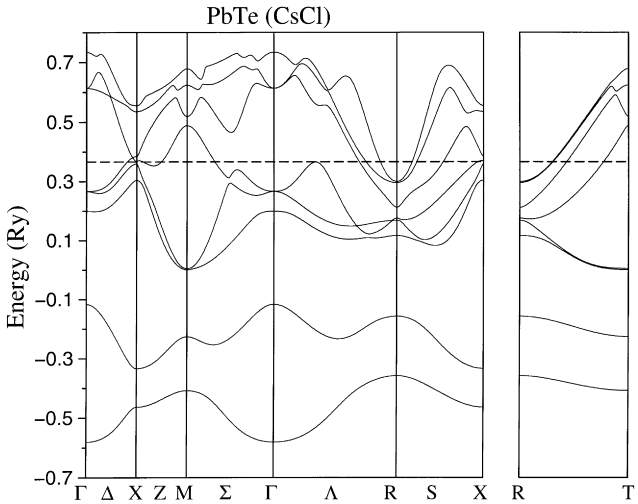

Fig. 5. The band structure along the symmetry lines of the BZ for PbTe in the (B2) structure at the lattice constant $a = 3.86$ Å. These bands were calculated using the SK Hamiltonian including the spin–orbit correlation.

for PbTe in the B2 structure contradict experiments which suggest that this structure is a metastable semiconductor.

Acknowledgements

The authors wish to thank M. Fornari for useful discussions about spin–orbit coupling. This research was supported by the US Office of Naval Research. This work was supported in part by a grant of HPC time from the DoD HPC Center, for computations on the IBM SP2 and SGI Origin at the Aeronautical Systems Center, Wright-Patterson Air Force Base, Dayton, OH.

Appendix A

Tables A1–A3

Table A1
SK Matrix including spin–orbit interaction

	$s_1\uparrow$	$p_{x1}\uparrow$	$p_{y1}\uparrow$	$p_{z1}\uparrow$	$s_2\uparrow$	$p_{x2}\uparrow$	$p_{y2}\uparrow$	$p_{z2}\uparrow$	$s_1\downarrow$	$p_{x1}\downarrow$	$p_{y1}\downarrow$	$p_{z1}\downarrow$	$s_2\downarrow$	$p_{x2}\downarrow$	$p_{y2}\downarrow$	$p_{z2}\downarrow$
$s_1\uparrow$	$H_{1,1}$	$G_{1,2}$	$G_{1,3}$	$G_{1,4}$	$H_{1,5}$	$G_{1,6}$	$G_{1,7}$	$G_{1,8}$	0	0	0	0	0	0	0	0
$p_{x1}\uparrow$	$G_{2,1}$	$H_{2,2}$	$H_{2,3}-i\lambda_1$	$H_{2,4}$	$G_{2,5}$	$H_{2,6}$	$H_{2,7}$	$H_{2,8}$	0	0	0	λ_1	0	0	0	0
$p_{y1}\uparrow$	$G_{3,1}$	$H_{3,2}+i\lambda_1$	$H_{3,3}$	$H_{3,4}$	$G_{3,5}$	$H_{3,6}$	$H_{3,7}$	$H_{3,8}$	0	0	0	$-i\lambda_1$	0	0	0	0
$p_{z1}\uparrow$	$G_{4,1}$	$H_{4,2}$	$H_{4,3}$	$H_{4,4}$	$G_{4,5}$	$H_{4,6}$	$H_{4,7}$	$H_{4,8}$	0	$-\lambda_1$	$i\lambda_1$	0	0	0	0	0
$s_2\uparrow$	$H_{5,1}$	$G_{5,2}$	$G_{5,3}$	$G_{5,4}$	$H_{5,5}$	$G_{5,6}$	$G_{5,7}$	$G_{5,8}$	0	0	0	0	0	0	0	0
$p_{x2}\uparrow$	$G_{6,1}$	$H_{6,2}$	$H_{6,3}$	$H_{6,4}$	$G_{6,5}$	$H_{6,6}$	$H_{6,7}-i\lambda_2$	$H_{6,8}$	0	0	0	0	0	0	0	λ_2
$p_{y2}\uparrow$	$G_{7,1}$	$H_{7,2}$	$H_{7,3}$	$H_{7,4}$	$G_{7,5}$	$H_{7,6}+i\lambda_2$	$H_{7,7}$	$H_{7,8}$	0	0	0	0	0	0	0	$-i\lambda_2$
$p_{z2}\uparrow$	$G_{8,1}$	$H_{8,2}$	$H_{8,3}$	$H_{8,4}$	$G_{8,5}$	$H_{8,6}$	$H_{8,7}$	$H_{8,8}$	0	0	0	0	0	$-\lambda_2$	$i\lambda_2$	0
$s_1\downarrow$	0	0	0	0	0	0	0	0	$H_{1,1}$	$G_{1,2}$	$G_{1,3}$	$G_{1,4}$	$H_{1,5}$	$G_{1,6}$	$G_{1,7}$	$G_{1,8}$
$p_{x1}\downarrow$	0	0	0	$-\lambda_1$	0	0	0	0	$G_{2,1}$	$H_{2,2}$	$H_{2,3}+i\lambda_1$	$H_{2,4}$	$G_{2,5}$	$H_{2,6}$	$H_{2,7}$	$H_{2,8}$
$p_{y1}\downarrow$	0	0	0	$-i\lambda_1$	0	0	0	0	$G_{3,1}$	$H_{3,2}-i\lambda_1$	$H_{3,3}$	$H_{3,4}$	$G_{3,5}$	$H_{3,6}$	$H_{3,7}$	$H_{3,8}$
$p_{z1}\downarrow$	0	λ_1	$i\lambda_1$	0	0	0	0	0	$G_{4,1}$	$H_{4,2}$	$H_{4,3}$	$H_{4,4}$	$G_{4,5}$	$H_{4,6}$	$H_{4,7}$	$H_{4,8}$
$s_2\downarrow$	0	0	0	0	0	0	0	0	$H_{5,1}$	$G_{5,2}$	$G_{5,3}$	$G_{5,4}$	$H_{5,5}$	$G_{5,6}$	$G_{5,7}$	$G_{5,8}$
$p_{x2}\downarrow$	0	0	0	0	0	0	0	$-\lambda_2$	$G_{6,1}$	$H_{6,2}$	$H_{6,3}$	$H_{6,4}$	$G_{6,5}$	$H_{6,6}$	$H_{6,7}+i\lambda_2$	$H_{6,8}$
$p_{y2}\downarrow$	0	0	0	0	0	0	0	$-i\lambda_2$	$G_{7,1}$	$H_{7,2}$	$H_{7,3}$	$H_{7,4}$	$G_{7,5}$	$H_{7,6}-i\lambda_2$	$H_{7,7}$	$H_{7,8}$
$p_{z2}\downarrow$	0	0	0	0	0	λ_2	$i\lambda_2$	0	$G_{8,1}$	$H_{8,2}$	$H_{8,3}$	$H_{8,4}$	$G_{8,5}$	$H_{8,6}$	$H_{8,7}$	$H_{8,8}$

Table A2
SK Matrix (real part). x, y, z should be multiplied by π

$H_{1,1}$	$A_1 + 4A_2[\cos(x)\cos(y) + \cos(y)\cos(z) + \cos(z)\cos(x)] + 2B_1[\cos(2x) + \cos(2y) + \cos(2z)]$
$H_{1,5}$	$2D_1[\cos(x) + \cos(y) + \cos(z)] + 8F_1\cos(x)\cos(y)\cos(z)$
$H_{2,2}$	$A_6 + 4A_7\cos(x)[\cos(y) + \cos(z)] + 4A_8\cos(y)\cos(z) + 2B_4\cos(2x) + 2B_5[\cos(2y) + \cos(2z)]$
$H_{2,3}$	$-4A_9\sin(x)\sin(y)$
$H_{2,4}$	$-4A_9\sin(x)\sin(z)$
$H_{2,6}$	$2D_4\cos(x) + 2D_5[\cos(y) + \cos(z)] + 8F_4\cos(x)\cos(y)\cos(z)$
$H_{2,7}$	$-8F_5\sin(x)\sin(y)\cos(z)$
$H_{2,8}$	$-8F_5\sin(x)\sin(z)\cos(y)$
$H_{3,3}$	$A_6 + 4A_7\cos(y)[\cos(z) + \cos(x)] + 4A_8\cos(z)\cos(x) + 2B_4\cos(2y) + 2B_5[\cos(2z) + \cos(2x)]$
$H_{3,4}$	$-4A_9\sin(y)\sin(z)$
$H_{3,6}$	$H_{2,7}$
$H_{3,7}$	$2D_4\cos(y) + 2D_5[\cos(z) + \cos(x)] + 8F_4\cos(x)\cos(y)\cos(z)$
$H_{3,8}$	$-8F_5\sin(y)\sin(z)\cos(x)$
$H_{4,4}$	$A_6 + 4A_7\cos(z)[\cos(x) + \cos(y)] + 4A_8\cos(x)\cos(y) + 2B_4\cos(2z) + 2B_5[\cos(2x) + \cos(2y)]$
$H_{4,6}$	$H_{2,8}$
$H_{4,7}$	$H_{3,8}$
$H_{4,8}$	$2D_4\cos(z) + 2D_5[\cos(y) + \cos(x)] + 8F_4\cos(x)\cos(y)\cos(z)$
$H_{5,5}$	$C_1 + 4C_2[\cos(x)\cos(y) + \cos(y)\cos(z) + \cos(z)\cos(x)] + 2E_1[\cos(2x) + \cos(2y) + \cos(2z)]$
$H_{6,6}$	$C_6 + 4C_7\cos(x)[\cos(y) + \cos(z)] + 4C_8\cos(y)\cos(z) + 2E_4\cos(2x) + 2E_5[\cos(2y) + \cos(2z)]$
$H_{6,7}$	$-4C_9\sin(x)\sin(y)$
$H_{6,8}$	$-4C_9\sin(x)\sin(z)$
$H_{7,7}$	$C_6 + 4C_7\cos(y)[\cos(z) + \cos(x)] + 4C_8\cos(z)\cos(x) + 2E_4\cos(2y) + 2E_5[\cos(2z) + \cos(2x)]$
$H_{7,8}$	$-4C_9\sin(x)\sin(z)$
$H_{8,8}$	$C_6 + 4C_7\cos(z)[\cos(x) + \cos(y)] + 4C_8\cos(x)\cos(y) + 2E_4\cos(2z) + 2E_5[\cos(2x) + \cos(2y)]$

Table A3
SK matrix (imaginary part). x, y, z should be multiplied by π

$G_{1,2}$	$-4A_3 \sin(x)[\cos(y) + \cos(z)] - 2B_2 \sin(2x)$
$G_{1,3}$	$-4A_3 \sin(y)[\cos(z) + \cos(x)] - 2B_2 \sin(2y)$
$G_{1,4}$	$-4A_3 \sin(z)[\cos(x) + \cos(y)] - 2B_2 \sin(2z)$
$G_{1,6}$	$+2D_2 \sin(x) + 8F_3 \sin(x) \cos(y) \cos(z)$
$G_{1,7}$	$+2D_2 \sin(y) + 8F_3 \sin(y) \cos(z) \cos(x)$
$G_{1,8}$	$+2D_2 \sin(z) + 8F_3 \sin(z) \cos(x) \cos(y)$
$G_{2,5}$	$-2D_3 \sin(x) - 8F_2 \sin(x) \cos(y) \cos(z)$
$G_{3,5}$	$-2D_3 \sin(y) - 8F_2 \sin(y) \cos(z) \cos(x)$
$G_{4,5}$	$-2D_3 \sin(z) - 8F_2 \sin(z) \cos(x) \cos(y)$
$G_{5,6}$	$-4C_3 \sin(x)[\cos(y) + \cos(z)] - 2E_2 \sin(2x)$
$G_{5,7}$	$-4C_3 \sin(y)[\cos(z) + \cos(x)] - 2E_2 \sin(2y)$
$G_{5,8}$	$-4C_3 \sin(z)[\cos(x) + \cos(y)] - 2E_2 \sin(2z)$

References

[1] D.L. Mitchell, R.F. Wallis, Phys. Rev. 151 (1966) 581.
[2] J.B. Conklin Jr., L.E. Johnson, G.W. Pratt, Phys. Rev. 137 (1965) A1282.
[3] S. Rabii, Phys. Rev. 167 (1968) 801.
[4] P.T. Bailey, Phys. Rev. 170 (1968) 723.
[5] H. Overhof, U. Rossler, Phys. Status Solidi 37 (1970) 691.
[6] F. Herman, R.L. Kortum, I.B. Ortenburger, J.P. Van Dyke, J. Phys. (Paris) 29 (1968) c4–62.
[7] G. Martinez, M. Schluter, M.L. Cohen, Phys. Rev. B 11 (1975) 651.
[8] G. Martinez, M. Schluter, M.L. Cohen, Phys. Rev. B 11 (1975) 660.
[9] P.J. Lin, K. Kleinman, Phys. Rev. 142 (1966) 478.
[10] R.L. Bernick, L. Kleinman, Solid State Commun. 8 (1970) 569.
[11] Y.W. Tung, M.L. Cohen, Phys. Rev. 180 (1969) 823.
[12] S. Wei, A. Zunger, Phys. Rev. B 55 (1997) 13 605–13 610.
[13] O.K. Andersen, Phys. Rev. B 12 (1975) 3060.
[14] D. Singh, H. KraKauer, C.S. Wang, Phys. Rev. B 34 (1986) 8391.
[15] I. Weinberg, J. Chem. Phys. 36 (1962) 1112.
[16] I. Weinberg, J. Chem. Phys. 39 (1963) 492.
[17] I. Weinberg, J. Callaway, Nuovo Cimento 24 (1962) 190.
[18] G. Nimtz, B. Schlicht, Narrow-Gap Semiconductors, Springer, New York, 1985.
[19] M. Baleva, E. Mateeva, Phys. Rev. B 50 (1994) 8893.
[20] H. Zogg, A. Fach, J. John, J. Masek, P. Muller, C. Paglino, W. Buttler, Opt. Engng 33 (1994) 1440.
[21] H. Preier, Appl. Phys. 20 (1979) 189.
[22] T.K. Chaudhuri, Int. J. Engng Res. 16 (1992) 481.
[23] A.F. Gibson, Proc. Phys. Soc. B 65 (1952) 378.
[24] L. Hedin, B.I. Lundquist, J. Phys. C 4 (1971) 2064.
[25] M.J. Mehl, J.E. Osburn, D.A. Papaconstantopoulos, B.M. Klein, Phys. Rev. B 41 (1990) 10 311.
[26] M. Mehl, B.M. Klein, D.A. Papaconstantopoulos, in: J.H. Westbrook, R.L. Fleischer (Eds.), Principles, Intermetallic Compounds, vol. 1, Wiley, 1995 (chap. 9).
[28] F. Herman, S. Skillman, Atomic Structure Calculations, Prentice-Hall, Englewood Cliffs, NJ, 1963.
[29] K.C. Hass, H. Ehrenreich, B. Velicky, Phys. Rev. B 27 (1983) 1088.
[30] J.C. Slater, G.F. Koster, Phys. Rev. 94 (1954) 1498.
[31] D.A. Papaconstantopoulos, Handbook of Electronic Structure of Elemental Solids, Plenum Press, New York, 1986.
[32] M.A. Keegan, New methodology for computationally efficient electronic structure calculations and database of electronic structure, PhD thesis, George Mason University, Virginia, 1998.
[33] F. Birch, J. Geophys. Res. 83 (1978) 1257.
[34] J.P. Perdew, A. Zunger, Phys. Rev. B 23 (1981) 5048.
[35] H.J.F. Jansen, A.J. Freeman, Phys. Rev. B 30 (1984) 561.
[36] R.W. Godby, M. Schulter, L.J. Sham, Phys. Rev. B 36 (1987) 6497.